ISSN 1063-780X, Plasma Physics Reports, 2007, Vol. 33, No. 11, pp. 930–941. © Pleiades Publishing, Ltd., 2007.
Original Russian Text © S.Yu. Bogdanov, G.V. Dreiden, V.S. Markov, G.V. Ostrovskaya, A.G. Frank, 2007, published in Fizika Plazmy, 2007, Vol. 33, No. 11, pp. 1014–1027.

PLASMA DYNAMICS

Holographic Interferometry Study of Two-Fluid Properties of the Plasma in Current Sheets Formed in Heavy Noble Gases

S. Yu. Bogdanov[a], G. V. Dreiden[b], V. S. Markov[a], G. V. Ostrovskaya[b], and A. G. Frank[a]

[a] *Prokhorov Institute of General Physics, Russian Academy of Sciences, ul. Vavilova 38, Moscow, 119991 Russia*
[b] *Ioffe Physicotechnical Institute, Russian Academy of Sciences, Politecknicheskaya ul. 36, St. Petersburg, 194021 Russia*

Received January 17, 2007; in final form, March 22, 2007

Abstract—Two-exposure holographic interferometry was used to study the structure of current sheets formed in three-dimensional magnetic configurations with a singular X line in heavy noble gases (Ar, Kr, and Xe). It is found that, in the presence of a longitudinal magnetic field $\mathbf{B}_Z$ directed along the X line, plasma sheets take on an unusual shape: they are tilted and asymmetric. Their asymmetry becomes more pronounced as the mass of a plasma ion increases—a manifestation of the two-fluid properties of the plasma. The observed effects can be attributed to additional forces arising due to the interaction of the longitudinal magnetic field $\mathbf{B}_Z$ with Hall currents excited in a plane perpendicular to the X line. A qualitative model describing plasma dynamics with allowance for the Hall effect and accounting for most of the experimentally observed effects is proposed.

PACS numbers: 52.30.Cv, 52.35.Vd, 42.40.Kw

DOI: 10.1134/S1063780X07110050

1. INTRODUCTION

This paper is devoted to studying the structure of current sheets formed in three-dimensional (3D) magnetic configurations with a singular X line in heavy noble gases (Ar, Kr, and Xe). Singular X lines are of fundamental importance for magnetic reconnection, because it is in the vicinity of these lines that current sheets form and magnetic reconnection occurs [1]. The magnetic field perpendicular to the X line has a saddle structure (see Fig. 1). When small perturbations of the initial equilibrium state propagate in the plasma, they cause finite effects in the vicinity of the X line due to cumulative processes. As a rule, the nonlinear stage of the evolution of such perturbations is concluded with the formation of a current sheet.

The simplest 3D magnetic configuration with an X line has the form

$$\mathbf{B} = \{B_x; B_y; B_z\} = \{hy; hx; B_z\}. \quad (1)$$

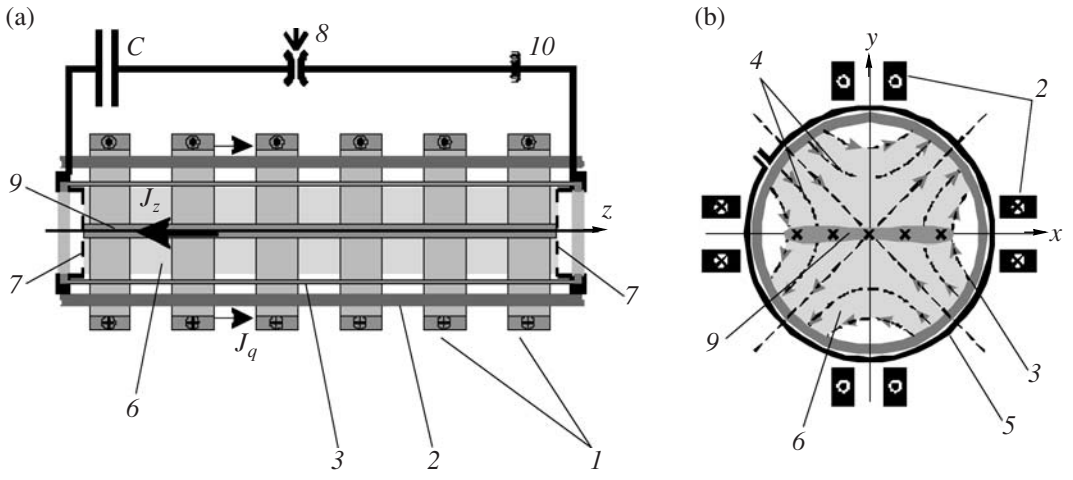

Fig. 1. (a) Longitudinal cross section of the CS-3D device in the (*y, z*) plane and (b) cross section in the (*x, y*) plane, perpendicular to the X line: (*1*) coils producing the uniform longitudinal field $\mathbf{B}_z$, (*2*) conductors producing the transverse magnetic field with a null line, (*3*) quartz vacuum chamber, (*4*) lines of the transverse magnetic field with a null line at the axis of the vacuum chamber, (*5*) coils of the Θ discharge for creating the initial plasma, (*6*) initial plasma, (*7*) end grid electrodes for the excitation of the electric current $\mathbf{J}_z$ in the plasma, (*8*) spark gap, (*9*) current sheet, and (*10*) Rogowski coil for measuring the current $\mathbf{J}_z$.

Here, the X line is aligned with the z axis, $B_z \approx$ const is the magnitude of the uniform longitudinal magnetic field $\mathbf{B}_z$ directed along the X line, and $h \approx$ const is the gradient of the transverse magnetic field in the (x, y) plane.

In [2, 3], we investigated the effect of the longitudinal magnetic field $\mathbf{B}_z$ on the process of plasma compression into a sheet and on the parameters of the formed plasma sheet. It was found that current sheets formed in heavy noble gases had an unusual structure: in the presence of a longitudinal field $\mathbf{B}_z$, the sheets produced in 3D magnetic field (1) become tilted and asymmetric. For the first time, these effects were observed in [4, 5], where current sheets were produced in an argon plasma. Asymmetric plasma sheets differed substantially from both sheets developing in an argon plasma in the absence of a longitudinal magnetic field ($B_z = 0$) [6–8] and those formed in 3D magnetic field (1) in a helium plasma [9]. An analysis of the plasma parameters showed that the observed asymmetry of plasma sheets was due to the two-fluid properties of the plasma, the generation of Hall currents in the (x, y) plane, and their interaction with the longitudinal magnetic field $\mathbf{B}_z$ [4, 10]. The subsequent experiments demonstrated that these effects become more pronounced as the mass of a plasma ion increases and that the character of asymmetry depends on the direction of the longitudinal magnetic field $\mathbf{B}_z$ [10–12].

Note that the first observations of the generation of Hall currents in current sheets produced under laboratory conditions were reported in [13, 14]. Recently, the generation of Hall currents in current sheets has attracted considerable attention. Phenomena of this kind were investigated in a number of experimental works [15–17], and the effect of the two-fluid properties of the plasma on the process of magnetic reconnection (in particular, as applied to the physics of the Earth's magnetosphere) is being actively studied theoretically (mostly by numerical simulations [18–26]).

The present paper is devoted to experimental studies of the structure of current sheets in successive stages of their evolution in 3D magnetic fields with an X line in plasmas of heavy noble gases (Ar, Kr, and Xe). The effect of the magnetic field topology on the spatiotemporal characteristics of plasma sheets, including their tilt and asymmetry, is investigated. A simple qualitative model of plasma dynamics with allowance for the Hall effect in a magnetic field with an X line is proposed and is used to analyze the experimental results.

2. EXPERIMENTAL STUDIES OF THE PLASMA IN CURRENT SHEETS FORMED IN PLASMAS OF HEAVY NOBLE GASES

2.1. Characteristic Features of the Structure of Plasma Sheets Formed in Plasmas of Heavy Noble Gases in a 3D Magnetic Field with an X line

The experimental layout and measurement technique (holographic interferometry) were the same as those used in our previous studies [2, 3, 9]. The formation and evolution of current sheets in 3D magnetic configurations with a singular X line were studied in the CS-3D device shown schematically in Fig. 1 [2, 9, 27, 28]. A characteristic feature of this device is that the parameters of a quasi-steady magnetic configuration, namely, the gradient of the transverse magnetic field h and the longitudinal magnetic field B_Z (see expression (1)), can be varied independently. Note that initial magnetic field (1) is uniform in the z direction. The plasma is produced in an 18-cm-diameter 100-cm-long cylindrical quartz vacuum chamber. The chamber is filled with a noble gas (He, Ar, Kr, or Xe) at a pressure of $p \approx$ 300 mTorr for helium and $p \approx 20$ mTorr for the other gases. The initial plasma in magnetic field (1) is produced by a Θ discharge with strong preionization. The uniformity of the initial plasma along the z axis is ensured by the uniform distribution of the loops of the Θ discharge throughout the length of the plasma gap (60 cm). A current sheet is generated by exciting a pulsed plasma current $\mathbf{J}_z$ directed parallel to the X line. Conditions under which a current sheet can form in the presence of a longitudinal magnetic field $\mathbf{B}_z$ were previously studied in [27–29].

The basic method for studying the structure of current sheets was holographic interferometry (see [2, 3, 9–11]). Holograms were recorded in the radiation of a ruby laser. The object beam propagated through the plasma exactly along the X line of magnetic field (1) (along the z axis, which was aligned with the axis of the vacuum chamber). Since the initial conditions are uniform in the z direction, it can be expected that the distribution of the plasma density N_e in the produced current sheet is also almost uniform along the z axis. In this case, the shifts of interference fringes in the recorded interferograms provide direct information on the spatial distribution of N_e in the (x, y) plane, which is perpendicular to the X line. Under our experimental conditions, the fringe shift equal to the distance between the neighboring fringes corresponds to an averaged (along the z axis) plasma density of $N_e = 5.33 \times 10^{15}$ cm^{-3}.

As noted above, our experiments with current sheets produced in an Ar plasma in 3D magnetic field (1) revealed a new effect: in the presence of a longitudinal field $\mathbf{B}_z$, plasma sheets took an unusual shape, namely, they became tilted and asymmetric about the x and y axes (see [2–5]).

Since effects of this kind were not observed when current sheets were formed in a He plasma [9], it was assumed that the tilt and asymmetry of plasma sheets was a manifestation of the two-fluid properties of the plasma and was due to the mass of an Ar ion being much greater than that of a He ion [2–5]. In order to verify this, we carried out experiments in which current sheets were produced in heavier noble gases, Kr and Xe [10, 11].

Figure 2 presents two series of holographic interferograms of plasma sheets formed in a Kr plasma in

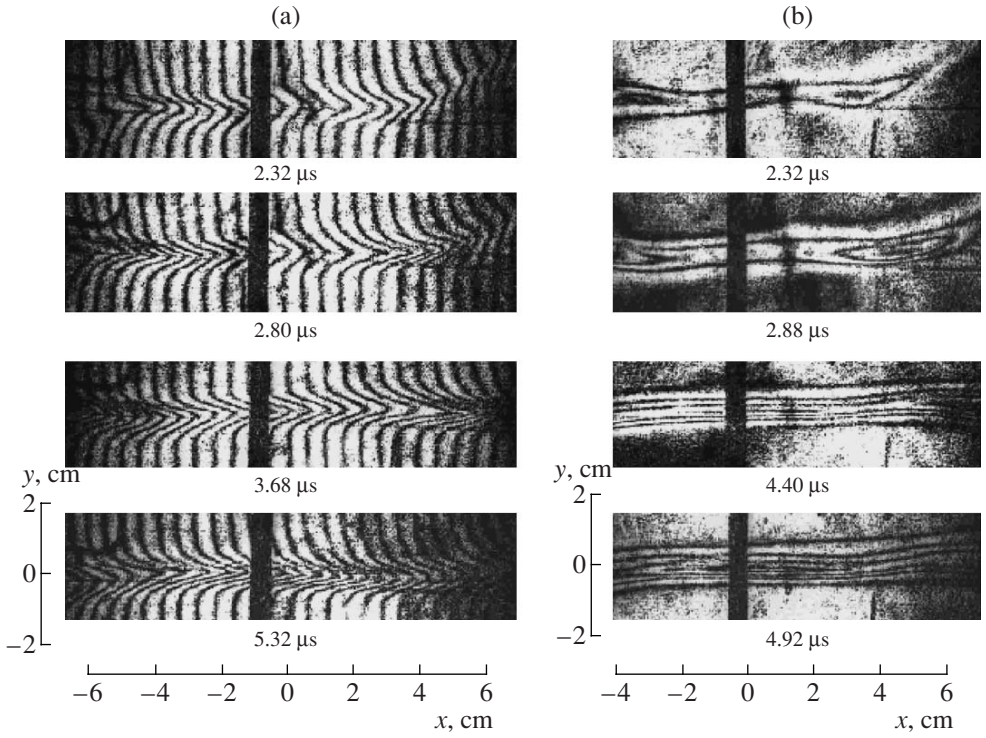

Fig. 2. Successive interferograms of a sheet produced in a Kr plasma at $h = 0.5$ kG/cm, $B_z = 1.43$ kG, and $J_z^{\max} = 70$ kA: (a) interferograms obtained in finite-width fringes and (b) those obtained in fringes of infinite width. The black band perpendicular to the sheet is the shadow of a tube with magnetic probes.

3D magnetic field (1). The interferograms correspond to successive instants of time t, counted from the beginning of the plasma current $\mathbf{J}_z$. The first series of interferograms (Fig. 2a) was obtained in finite-width fringes, whereas the second series (Fig. 2b) was obtained in fringes of infinite width. In the latter case, the interference fringes correspond to contour lines of the electron density and the difference in the electron density between two neighboring fringes is $\delta N_e = 5.33 \times 10^{15}$ cm^{-3}. Such interferograms visualize the plasma structure in successive stages of the sheet evolution. In contrast to plasma sheets formed in the absence of a longitudinal magnetic field $\mathbf{B}_z$, the sheets shown in Fig. 2 are asymmetric about the $x = 0$ and $y = 0$ planes. The deviation from the plane symmetry is most pronounced in the early stage of the sheets evolution and at the side edges of the sheet, far from the X line. The sheets are seen to be not only tilted to the x axis but also curved.

That sheets are curved can be seen even more clearly in interferograms of plasma sheets formed in Xe (Fig. 3). It is seen that, in the early stage of the sheet evolution, the edges of the sheet are tilted more strongly than its axial region.

The effect of the mass of a plasma ion on the sheet structure is illustrated in Fig. 4, which shows 2D spatial distributions of the electron density $N_e(x, y)$ in sheets formed in different gases (He, Ar, Kr, and Xe). The difference in the electron density between neighboring contour lines is $\delta N_e = 2 \times 10^{15}$ cm^{-3}. Holographic interferograms used to construct the distributions $N_e(x, y)$ were obtained for the same topology of magnetic field (1) ($h = 0.57$ kG/cm and $B_z = 2.9$ kG), the same maximum plasma current ($J_z = 70$ kA), and the same instant of time ($t \approx 3$ μs). However, the initial gas pressures in the vacuum chamber differed substantially: $p \approx 300$ mTorr for He and $p \approx 20$ mTorr for other gases. It can be seen from Fig. 4 that an increase in the atomic weight of the working gas (from $A = 4$ for He to $A = 131$ for Xe) is accompanied by a substantial increase in the angle at which the sheet is tilted with respect to the $y = 0$ plane. The electron density distribution in the sheet formed in He (Fig. 4a) is symmetric about the $y = 0$ plane and differs only slightly from distributions observed in 2D magnetic fields with $B_z = 0$. The side edges of a sheet formed in Ar ($A = 40$) are bent appreciably in opposite directions with respect to the $y = 0$ plane (Fig. 4b). This effect is even more pronounced for sheets formed in Kr and Xe (Figs. 4c, 4d). Note that, at the side edges of the sheet, the regions where N_e reaches its maximum are shifted in opposite directions along the y axis (Figs. 4c, 4d).

This effect is also observed in Fig. 5, which shows the electron density profiles $N_e(y)$ (along the sheet thickness) measured both in the central region of the sheet (at $x = 0$) and at its edges (at $x = \pm 4.5$ cm). The

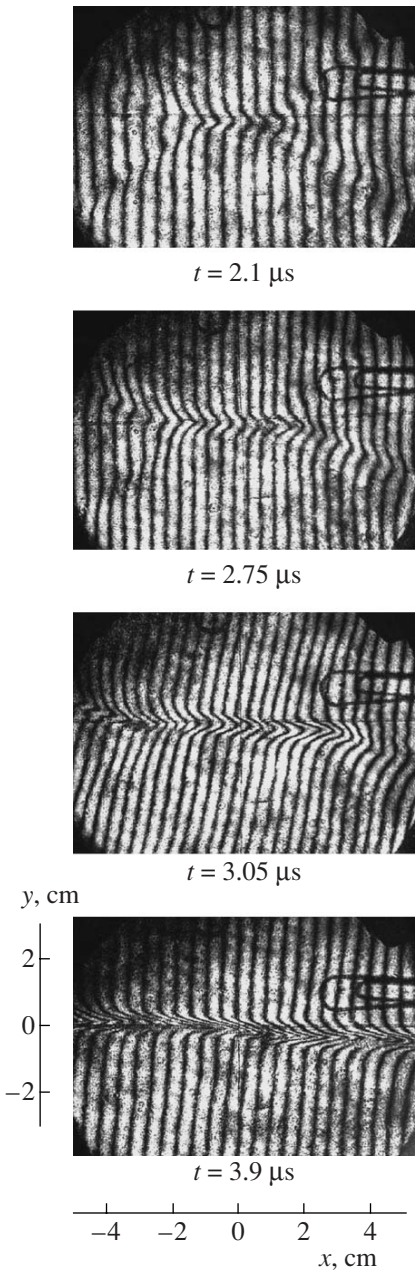

Fig. 3. Successive interferograms of a sheet produced in a Xe plasma at h = 0.57 kG/cm, B_z = 2.1 kG, and $J_z^{\max}$ = 70 kA.

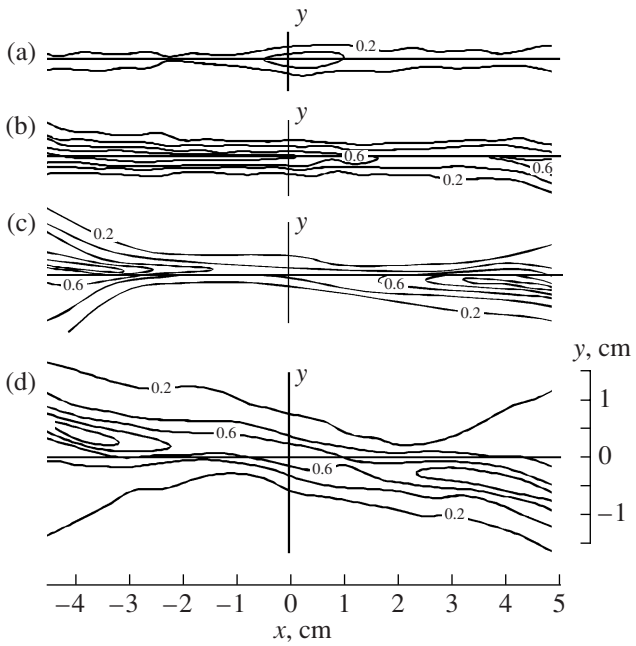

Fig. 4. Plasma sheets produced in plasmas of different gases: (a) He (A = 4), (b) Ar (A = 40), (c) Kr (A = 84), and (d) Xe (A = 131) (h = 0.57 kG/cm, B_z = 2.9 kG, $J_z^{\max}$ = 70 kA, $t \approx 3$ μs).

profiles $N_e(y)$ measured at the edges of sheets formed in Kr and Xe are not only shifted in opposite directions from the x axis but are also asymmetric about their peak values $N_e^{\max}$. It can be seen from Fig. 5 that, in sheets formed in He, the peaks of N_e are practically unshifted. In sheets formed in Ar, the shift is less than 2 mm, but in sheets produced in Kr and Xe, the shift reaches 4–6 mm. At the same time, the profiles $N_e(y)$ measured at the center of the sheet (at $x = 0$) are symmetric and their maxima lie at the x axis for all of the sheets formed in both He and heavy noble gases.

Thus, as the atomic weight of the working gas (and, accordingly, the ion mass) increases, the edges of the sheet shift by a progressively increasing distance from the $y = 0$ plane and the density profiles $N_e(y)$ at the sheet edges become more asymmetric.

Figures 4 and 5 also demonstrate another dependence of the sheet structure on the sort of noble gas. In sheets formed in a He plasma, the electron density is maximum at the center of the sheet (at $x = 0$, $y = 0$) and decreases monotonically toward its edges. In an Ar plasma, the density distribution $N_e(x)$ over the sheet width is more flattened and the peak values of $N_e(y)$ measured at the center and edges of the sheet (at $x = 0$ and $x = \pm 4.5$ cm, respectively) lie within the range $(6–8) \times 10^{15}$ cm^{-3}. Finally, sheets formed in Kr and Xe are characterized by the presence of two maxima of N_e at the sheet edges, the electron density in this maxima being substantially higher than at the center of the sheet (at $x = 0$, $y = 0$). Thus, as the atomic weight of the working gas increases, a unimodal distribution of the electron density over the sheet width (for He) changes to a double-hump distribution (for Kr and Xe). Double-hump distributions are typical of plasma sheets formed in Kr and Xe both in the presence of a longitudinal magnetic field $\mathbf{B}_z$ and in 2D magnetic configurations (i.e., at $B_z = 0$) [3].

Note also that the electron density in the central region of the sheet is almost the same for sheets formed

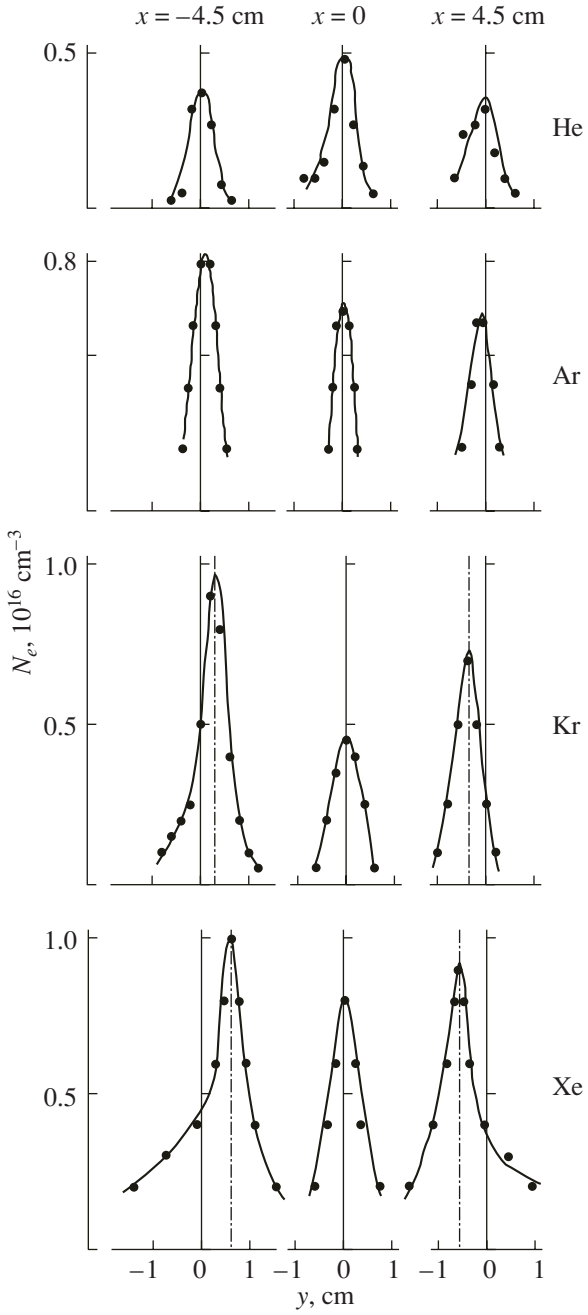

Fig. 5. Electron density profiles $N_e(y)$ measured in the centers of plasma sheets ($x = 0$) and at their side edges ($x = \pm 4.5$ cm) at $t \approx 3$ μs. The sheets were produced in different noble gases (He, Ar, Kr, and Xe) at $h = 0.57$ kG/cm, $B_z = 2.9$ kG, and $J_z^{\max} = 70$ kA.

in different noble gases and is equal to $(5–7) \times 10^{15}$ cm^{-3}. Hence, neither the 15-fold difference in the initial gas pressure (between He and the other gases) nor more than 30-fold difference in the ion mass (between He and Xe) affect the value of N_e at the center of the sheet. In agreement with our previous results (see [2, 3]), this value depends primarily on the plasma current $\mathbf{J}_z$

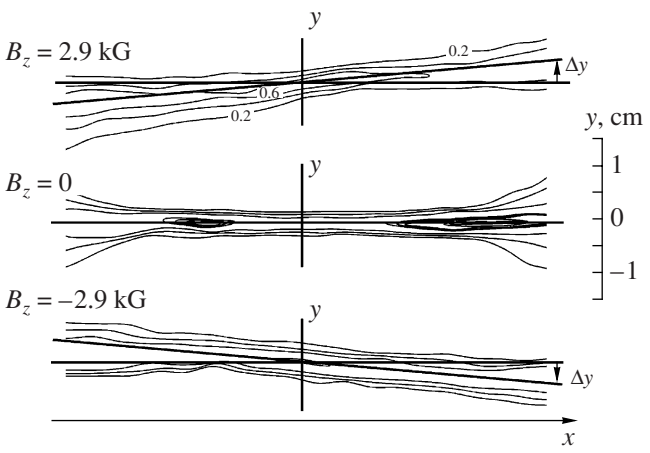

Fig. 6. Plasma sheets produced in a Kr plasma at two opposite directions of the longitudinal magnetic field $B_z = \pm 2.9$ kG and at $B_z = 0$ ($h = 0.57$ kG/cm, $J_z = 70$ kA, $t \approx 3$ μs).

directed along the X line and on the topology of magnetic field (1), i.e., on the values of B_z and h.

2.2. Effect of the Longitudinal Magnetic Field on the Tilt and Asymmetry of a Plasma Sheet

The effect of the magnetic field topology on the process of plasma compression into a sheet and on the parameters of the formed current sheet was thoroughly examined in [2, 3, 9]. Here, we only consider the effect of the longitudinal and transverse components of a 3D magnetic field on the tilt of a plasma sheet.

Figure 6 illustrates the effect of the direction of the longitudinal magnetic field $\mathbf{B}_z$ on the tilt of a sheet formed in a Kr plasma. It is clearly seen that the shifts of the sheet edges Δy from the $y = 0$ plane, which are indicated by arrows in Fig. 6, change their signs when the direction of the longitudinal field $\mathbf{B}_z$ is reversed. In the absence of a longitudinal component (at $B_z = 0$), i.e., in 2D magnetic fields, these shifts are absent.

Figure 7 shows the sheet tilt averaged over the sheet width as a function of B_z. As a measure of the sheet tilt, we used the shift Δy of the peak of the profile $N_e(y)$ (see Fig. 6) with respect to the x axis at a distance $x = \pm 5$ cm from the center of the sheet. The sheet was produced in a Kr plasma, the transverse field gradient was $h = 0.57$ kG/cm, and the longitudinal magnetic field was varied from 0 to 5.7 kG. The data presented in Fig. 7 refer to $t \approx 3$ μs. It can be seen that the sheet tilt first grows linearly with increasing B_z; however, at $B_z > 2.9$ kG, the growth slows down and then saturates. For sheets formed in Xe, an increase in B_z is accompanied not only by a change in the tilt angle at the sheet edges but also by the deformation of the electron density distribution $N_e(y)$ across the sheet. In this case, the sheet has a rather complicated structure, so it is difficult to unambiguously determine the dependence of the average tilt angle of the sheet on B_z.

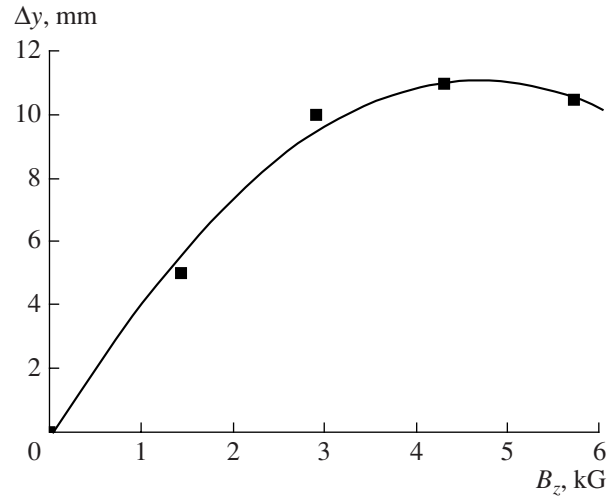

Fig. 7. Shift Δy of a plasma sheet from the midplane $y = 0$ at $x = \pm 5$ cm as a function of the longitudinal magnetic field B_z. The sheet was produced in a Kr plasma at $h =$ 0.57 kG/cm, and $J_z^{\max} = 70$ kA ($t \approx 3$ μs).

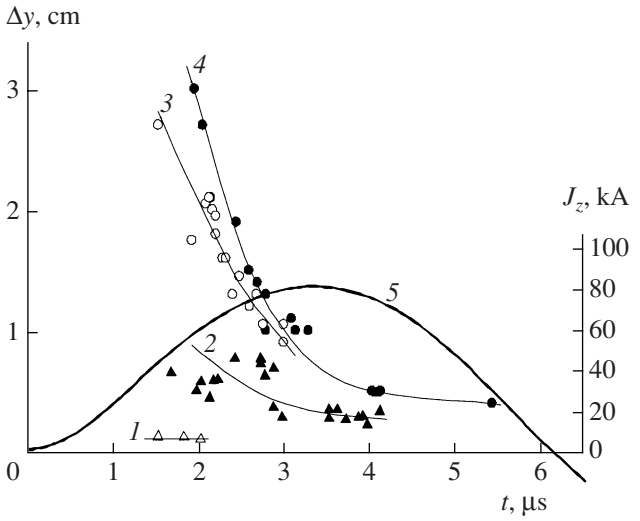

Fig. 8. Time dependences of the shifts Δy of plasma sheets from the midplane $y = 0$ at $x = \pm 5$ cm (curves *1–4*). Curve *5* shows the time dependence of the plasma current J_z. The sheets were produced in (*1*) He, (*2*) Ar, (*3*) Kr, and (*4*) Xe at $h = 0.57$ kG/cm and $B_z = 2.9$ kG.

The absolute value of the transverse field gradient h has little or no influence on the sheet tilt: the effect lies within the error of measurements of Δy (Fig. 9).

In some experiments, we changed both the sign of the gradient h and the direction of the plasma current $\mathbf{J}_z$. In this case, the tilt angle of the sheet remained unchanged. (Note that, in order for the spatial orientation of the sheet not to change, i.e., for the sheet to be extended along the x axis, the signs of h and J_z should both be changed simultaneously.)

2.3. Time Evolution of the Structure of Plasma Sheets in a 3D Magnetic Field

The spatiotemporal evolution of a plasma sheet can be traced from a series of interferograms obtained for a sheet formed in Kr (Figs. 2a, 2b). The interferograms refer to successive instants of time t counted from the beginning of the plasma current $\mathbf{J}_z$. It can be seen that the sheet tilt decreases with time and that it is nonuniform over the sheet width: the tilt is maximum at the sheet edges, whereas the central region of the sheet (in particular, in the late stage of its evolution) is almost parallel to the x axis. A similar behavior can also be observed in a series of interferograms illustrating the formation of a current sheet in a Xe plasma (see Fig. 3).

Curves *1–4* in Fig. 8 show the time dependences of the average tilt of plasma sheets formed in different gases (He, Ar, Kr, and Xe), and curve *5* shows the time dependence of the current J_z integrated over the cross section of the plasma sheet. It can be seen that the sheet tilt decreases rapidly with time for all of the gases under study. The greater the atomic mass of the working gas, the longer the time during which the sheet is tilted. The tilt of a sheet formed in He (curve *1*) becomes negligibly small as early as at 1.5–2 μs, whereas for heavy gases (Kr and Xe), the sheet tilt remains appreciable up to 4–5 μs (curves *3* and *4*).

Figure 9 shows the time dependence of the tilt for sheets formed in Kr for three different values of the transverse field gradient h in the range 0.42–0.57 kG/cm. It can be seen that the sheet tilt decreases fairly rapidly with time; in this case, however, the shift

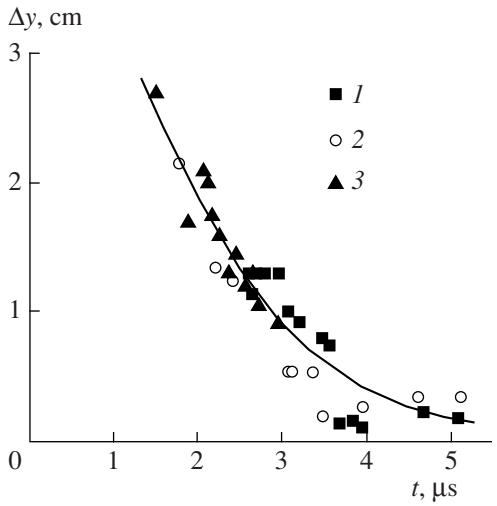

Fig. 9. Time dependences of the shifts Δy of plasma sheets from the midplane $y = 0$ at $x = \pm 5$ cm. The sheets were produced in Kr at $B_z = 2.9$ kG, $J_z^{\max} = 70$ kA, and different values of the transverse field gradient h: (*1*) 0.42, (*2*) 0.50, and (*3*) 0.57 kG/cm.

of the sheet edge depends only slightly on h in the range of gradients under study.

2.4. Summary

The data obtained in our experiments on studying the structure of plasma sheets formed in 3D magnetic fields with an X line (1) can be summarized as follows:

(i) Plasma sheets formed in heavy noble gases (Ar, Kr, and Xe) in the presence of a longitudinal component magnetic field B_z are found to be tilted and asymmetric, whereas in sheets formed in He and also at $B_z = 0$, these effects were absent.

(ii) It is shown that the tilt and asymmetry of plasma sheets increase substantially with increasing ion mass (see Figs. 4, 5).

(iii) The tilt angle changes its sign when the direction of the longitudinal magnetic field $\mathbf{B}_z$ is reversed (Fig. 6). An increase in the absolute value of $\mathbf{B}_z$ is accompanied by a linear growth of the sheet tilt; this growth, however, slows down at large values of B_z (Fig. 7).

(iv) Within the range of initial conditions under study, a change in the transverse field gradient h only slightly affects the tilt of a plasma sheet.

(v) The tilt and asymmetry of plasma sheets are most pronounced in the early stages of their formation and also near the sheet edges (Figs. 2, 3).

(vi) For plasma sheets formed in all of the gases under study, the sheet tilt is found to decrease with time (Fig. 8). The greater the atomic mass of the working gas, the longer the time during which the sheet is tilted.

The obtained experimental data, first of all, the fact that the tilt and asymmetry of plasma sheets increase with ion mass, indicate a significant role of two-fluid properties of the plasma, which probably give rise to additional forces resulting in the sheet deformation.

3. DISCUSSION AND INTERPRETATION OF THE RESULTS

3.1. Electrodynamic Forces Acting on a Plasma in a 3D Magnetic Field with an X line with Allowance for Hall Currents

The formation of a current sheet in a 2D magnetic configuration with an X-type null line ($B_z = 0$; see Eq. (1)) was thoroughly examined in the MHD approximation in [1, 30, 31]. When the plasma current $\mathbf{J}_z$ is excited in the direction parallel to the X line, perturbations of the magnetic field initially appear near the side boundaries of the plasma and then propagate in the radial direction with a local Alfvén velocity v_A from the plasma boundaries toward the X line. The velocity v_A depends on the strength of the transverse magnetic field $\mathbf{B}_\perp$, the plasma ion density N_i, and the ion mass M_i:

$$v_A = \frac{|\mathbf{B}_\perp|}{(4\pi N_i M_i)^{1/2}}. \quad (2)$$

As the X line is approached, the propagation velocity of perturbations, v_A, decreases because the value of $|\mathbf{B}_\perp|$ decreases (see expression (1)), whereas the amplitude of magnetic field perturbations and, accordingly, the current density j_z increase [32, 33]. Near the X line, magnetic field perturbations can become comparable with and even larger than the magnetic field of initial configuration (1). This nonlinear stage is concluded with the formation of a current sheet. The magnetic structure of the formed current sheet usually differs substantially from the structure of the initial magnetic field [34, 33]. The formation of a current sheet is accompanied by efficient compression of the plasma into a sheet, in which the electron density usually exceeds the initial plasma density by a factor of 10–15 (see [2, 3, 6–8]).

The excitation of the current $\mathbf{j}_z$ in magnetic field (1) gives rise to the Ampère forces in the (x, y) plane,

$$\mathbf{f}^{(1)} = \frac{1}{c}\mathbf{j}_z \times \mathbf{B}_\perp, \quad (3)$$

which set the plasma into motion. Figure 10a schematically shows forces $\mathbf{f}^{(1)}$ arising in the initial stage of the process, when the perturbation wave has not yet reached the X line (the front of the propagating wave is shown by the dashed line). In this stage, the plasma currents are relatively low and only slightly disturb initial magnetic field (1). The field of forces $\mathbf{f}^{(1)}$ is symmetric about the $x = 0$ and $y = 0$ planes, the force $\mathbf{f}^{(1)}$ at each point being directed normally to the transverse magnetic field $\mathbf{B}_\perp$. It can be seen in Fig. 10a that the y components of the forces $\mathbf{f}^{(1)}$ are directed from the outer regions toward the midplane $y = 0$, whereas the x components of the forces $\mathbf{f}^{(1)}$ are directed outward from the plane $x = 0$. It is under the action of these forces that a current sheet forms near the $y = 0$ plane and the plasma is compressed into a sheet.

If the electric current $\mathbf{j}$ flows in the plasma, then the electron and ion velocities, $\mathbf{v}_e$ and $\mathbf{v}_i$, should differ from one another:

$$\mathbf{j} = eN_e(\mathbf{v}_i - \mathbf{v}_e). \quad (4)$$

Such a plasma should be described by the generalized Ohm law allowing for the two-fluid nature of the plasma [35–41]. For a quasineutral plasma, ignoring the electron inertia, the generalized Ohm law can be written in the following form:

$$\mathbf{j} = \sigma\left(\mathbf{E} + \frac{1}{c}\mathbf{v}_i \times \mathbf{B} + \frac{\nabla p_e}{eN_e} - \frac{1}{eN_e c}\mathbf{j} \times \mathbf{B}\right). \quad (5)$$

Here, $\sigma = N_e e^2 \tau_e / m$ is the plasma conductivity, e and m are the charge and mass of an electron, τ_e is the mean free time between Coulomb collisions of electrons with plasma ions (or between scattering by plasma fluctuations in a turbulent plasma), and p_e is the electron pressure.

The first two terms in the brackets on the right-hand side of Eq. (5) correspond to the electric field in the frame of reference moving with the average mass velocity, which is approximately equal to the ion flow velocity $\mathbf{v} \approx \mathbf{v}_i$; the third term is related to the electron-pressure gradient; and the last term is due to the Hall effect. In generalized Ohm law (5), the two-fluid nature of the plasma is accounted for through the last two terms, which are usually of the same order of magnitude. If the macroscopic plasma velocity $\mathbf{v}$ is high enough, ($|\mathbf{v}_i| \gg |\mathbf{j}/eN_e|$), i.e., if the second term in Eq. (5) exceeds the last two terms, then the conventional MHD approximation is sufficient for describing such a plasma. When the opposite inequality holds, i.e., when the ion velocity is lower than the current velocity or the electron velocity,

$$|\mathbf{v}_i| < \left|\frac{\mathbf{j}}{eN_e}\right|, \tag{6}$$

it is necessary to take into account the two-fluid effects.

Estimates based on direct measurements of the magnetic field in Ar and Kr plasmas [33] show that, in the stage in which perturbations propagate from the plasma boundaries toward the X line, the current velocity $u_c = j/eN_e$ gradually increases and can become comparable with v_A, which is larger than the ion velocity v_i by a factor of 2–4. Hence, already in the initial stage preceding the formation of a current sheet, the two-fluid effects must be taken into consideration. Since the directed ion velocity is low and the plasma density gradients are absent in this stage, we can ignore the second and third terms in Eq. (5). The last term in Eq. (5), which is related to the Hall effect, clearly indicates that the plasma current can have components oriented perpendicular to the applied electric field and to the current that is initiated by this field. In other words, the excitation of the currents $\mathbf{j}_z$ in the plasma can lead to the generation of Hall currents in the (x, y) plane,

$$\mathbf{j}^{(H)} = -\frac{\sigma}{ceN_e}\mathbf{j}_z \times \mathbf{B}_\perp, \tag{7}$$

which arise due to the motion of electrons relative to the low-mobility heavy ions. At each point, the Hall currents are directed oppositely to the vector $\mathbf{f}^{(1)}$ (see Eq. (3)):

$$\mathbf{j}^{(H)} = -\frac{\omega_e \tau_e}{B}\mathbf{j}_z \times \mathbf{B}_\perp = -c\frac{\chi}{B}\mathbf{f}^{(1)}. \tag{7a}$$

Here, $\omega_e = eB/mc$ is the electron cyclotron frequency and $\chi = \omega_e \tau_e$ is the so-called Hall parameter [41], which characterizes the degree to which the plasma electrons are magnetized. It follows from formula (7a) that, taking into account that $\mathbf{j}^{(H)}$ and $\mathbf{f}^{(1)}$ are oppositely directed, the structure of the Hall currents in the initial stage of the process can be schematically described by the diagram shown in Fig. 10a.

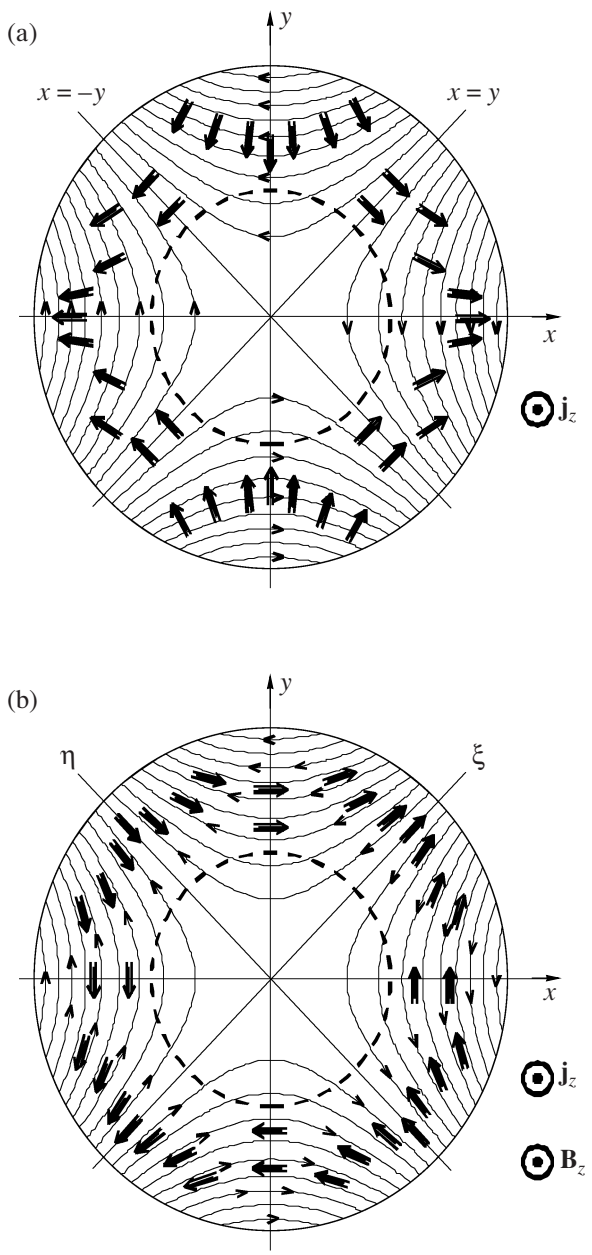

Fig. 10. Structure of electrodynamic forces (arrows) governing the plasma dynamics in the (x, y) plane in 3D magnetic field (1) with an X line in the initial stage of the current sheet evolution: (a) forces $\mathbf{f}^{(1)}$, arising due to the interaction of the current $\mathbf{j}_z$ with the transverse magnetic field $\mathbf{B}_\perp$, and (b) forces $\mathbf{f}_\perp^{(H)}$, arising due to the interaction of the Hall currents with the longitudinal magnetic field $\mathbf{B}_z$. The lines of the transverse magnetic field $\mathbf{B}_\perp$ are shown by light solid lines, and the front of the perturbation wave propagating from the plasma boundaries toward the X line is shown by the dashed line.

In turn, the interaction of the Hall currents $\mathbf{j}^{(H)}$ with the 3D magnetic field $\mathbf{B}$ gives rise to additional Ampère forces

$$\mathbf{f}^{(H)} = \frac{1}{c}\mathbf{j}^{(H)} \times \mathbf{B} = -\frac{\chi}{B}\mathbf{f}^{(1)} \times \mathbf{B}, \quad (8)$$

which are directed perpendicular to both the magnetic field $\mathbf{B}$ and the force $\mathbf{f}^{(1)}$. Using formula (3) for $\mathbf{f}^{(1)}$, expression (8) can be rewritten in the form

$$\mathbf{f}^{(H)} = -\frac{\chi}{cB}(\mathbf{j}_z \times \mathbf{B}_\perp) \times \mathbf{B}. \quad (8a)$$

Representing the magnetic field $\mathbf{B}$ as a sum of the transverse and longitudinal components, $\mathbf{B} = \mathbf{B}_\perp(x, y) + \mathbf{B}_z$, and transforming the triple vector product in expression (8a), we find

$$\mathbf{f}^{(H)} = \frac{\chi}{cB}\{\mathbf{j}_z(B_\perp)^2 - \mathbf{B}_\perp(\mathbf{B}_z \cdot \mathbf{j}_z)\}. \quad (9)$$

Hence, the Ampère forces $\mathbf{f}^{(H)}$, which arise from the interaction of the Hall currents with the 3D magnetic field, have two components, one of which is directed along the z axis, whereas the other lies in the (x, y) plane. The first term on the right-hand side of Eq. (9) corresponds to the z component of the force $\mathbf{f}^{(H)}$, which is independent of the longitudinal magnetic field $\mathbf{B}_z$ and, consequently, can exist in a 2D magnetic field (at $B_z = 0$). This component of the force $\mathbf{f}^{(H)}$ can give rise to motions in the z direction without breaking the symmetry of the flows in the (x, y) plane.

The second component of the force $\mathbf{f}^{(H)}$, which lies in the (x, y) plane, is equal to

$$\mathbf{f}_\perp^{(H)} = -\frac{\chi}{cB}\mathbf{B}_\perp(\mathbf{B}_z \cdot \mathbf{j}_z). \quad (9a)$$

Obviously, the force $\mathbf{f}_\perp^{(H)}$ can arise only in the presence of a longitudinal magnetic field $\mathbf{B}_Z$. The direction of the vector $\mathbf{f}_\perp^{(H)}$ at each spatial point can either be directed oppositely to the transverse field $\mathbf{B}_\perp(x, y)$ (if the vectors $\mathbf{B}_z$ and $\mathbf{j}_z$ are unidirectional) or coincide with the direction of $\mathbf{B}_\perp(x, y)$ (if the vectors $\mathbf{B}_z$ ad $\mathbf{j}_z$ are directed oppositely).

Figure 10b shows the structure of the force field $\mathbf{f}_\perp^{(H)}$ in the initial stage of evolution, when the plasma currents are still low and do not cause substantial perturbations in initial magnetic field (1). Note that, unlike the force field $\mathbf{f}^{(1)}$, the force field $\mathbf{f}_\perp^{(H)}$ is asymmetric about the planes $x = 0$ and $y = 0$. It should be noted, however, that the force field $\mathbf{f}_\perp^{(H)}$ is always symmetric about both separatrix planes of the transverse magnetic field: $x = y$ and $x = -y$ (Fig. 10b). It can easily be shown that the force field $\mathbf{f}_\perp^{(H)}$ represented in the (ξ, η) coordinates, rotated counterclockwise by 45° with respect to the (x, y) coordinates, is identical in structure to the force field $\mathbf{f}^{(1)}$ represented in the (x, y) coordinates. In other words, the force field $\mathbf{f}_\perp^{(H)}$ differs from the force field $\mathbf{f}^{(1)}$ in the angular orientation with respect to the (x, y) plane and also in the absolute values of $f_\perp^{(H)}$ and $f^{(1)}$. The sense of rotation of the force field $\mathbf{f}_\perp^{(H)}$ as a whole by ±45° with respect to the force field $\mathbf{f}^{(1)}$ (either clockwise or counterclockwise) depends on the direction of the longitudinal component of the magnetic field $\mathbf{B}_z$.

As was noted above, when $|\mathbf{f}^{(1)}| \gg |\mathbf{f}_\perp^{(H)}|$, a current sheet forms near the $y = 0$ plane and regions with an increased plasma density form just in the vicinity of this plane (Fig. 10a). However, when $|\mathbf{f}_\perp^{(H)}| \gg |\mathbf{f}^{(1)}|$, regions with an increased plasma density should be located near one of the separatrix planes, i.e., they should be rotated by 45° with respect to the $y = 0$ plane, either clockwise or counterclockwise.

For the directions of the magnetic fields and currents corresponding to Fig. 10b, the forces $\mathbf{f}_\perp^{(H)}$ near the $\xi = 0$ plane (which corresponds to the separatrix plane $x = -y$ in Fig. 10a) are directed toward the X line, i.e., toward the center of the system, whereas near the $\eta = 0$ plane (which corresponds to the separatrix plane $x = y$), the forces $\mathbf{f}_\perp^{(H)}$ are directed outward. Plasma flows that arise under the action of these forces should increase the plasma density near the $\eta = 0$ plane, by analogy with the plasma compression near the $y = 0$ plane when the flows are induced by the forces $\mathbf{f}^{(1)}$ (see Fig. 10a).

Hence, an analysis of the two limiting cases shows that the maximum possible difference between the angular orientations of the regions with an increased plasma density is 45°. Actually, the forces $\mathbf{f}^{(1)}$ and $\mathbf{f}_\perp^{(H)}$ in the (x, y) plane act on the plasma simultaneously and the angle by which the plane containing the regions with an increased plasma density is rotated relative to the $y = 0$ plane should lie between 0° and 45°, depending on particular conditions.

Let us estimate the relative role of the forces $\mathbf{f}^{(1)}$ and $\mathbf{f}_\perp^{(H)}$. According to expressions (3) and (9a), the absolute values of these forces are equal to $f^{(1)} = j_z B_\perp/c$ and $f_\perp^{(H)} = j_z B_\perp(\chi B_z/Bc)$, so their ratio is

$$\frac{f_\perp^{(H)}}{f^{(1)}} = \chi\frac{B_z}{B} = \chi_Z, \quad (10)$$

where $\chi_Z = \tau_e\omega_e(B_z)$ and $\omega_e(B_z)$ is the electron cyclotron frequency in the longitudinal magnetic field $\mathbf{B}_z$. Hence, the force $\mathbf{f}_\perp^{(H)}$ can make a substantial contribution to the plasma dynamics when the Hall parameter χ_z, characterizing the degree to which electrons are magnetized in

the field $\mathbf{B}_z$, is high enough: $\chi_z > 1$. Obviously, the resultant of these forces at each point of the (x, y) plane is rotated relative to the vector $\mathbf{f}^{(1)}$ by a certain angle φ whose tangent is also defined by ratio (10), i.e., by the degree to which electrons are magnetized in the field $\mathbf{B}_z$:

$$\tan\varphi(x, y) = \frac{f_\perp^{(H)}}{f^{(1)}} = \chi_z. \quad (10a)$$

In magnetic configuration (1), the angle by which the symmetry plane of the field of the resultant forces is rotated relative to the $y = 0$ plane is half as large:

$$\Psi = \frac{1}{2}\arctan(\chi_z), \quad (11)$$

which can easily be seen from geometrical considerations.

Note that the above analysis of the Hall currents and the forces resulting from the interaction of these currents with the magnetic field applies not only to the initial stage of propagation of perturbations in field (1) but also to the subsequent stages in which the magnetic field configuration changes substantially due to the development of a current sheet.

3.2. Discussion of the Experimental Results

The above qualitative analysis of the structure and features of electrodynamic forces acting on the plasma in a 3D magnetic field with an X line in the presence of Hall currents allows us to explain most of the experimental results obtained in this study. Among these results is a change in the sheet tilt when the direction of the longitudinal magnetic field $\mathbf{B}_z$ is reversed (Fig. 6) and the fact that the tilt does not depend on the transverse component of the magnetic field (Fig. 9) (the latter is explained by the quantity χ_z being independent of $B_\perp$). From expression (11), it is also easy to explain the experimentally observed dependence of the tilt angle on B_z (Fig. 7). Indeed, at small values of the parameter χ_z, the tilt angle is $\Psi \approx 0.5\chi_Z$ (i.e., it is proportional to B_z), whereas at $\chi_z \gg 1$, the angle Ψ depends only slightly on B_z and is close to45°.

If the ratio χ_z remained constant in both time and space, then the field of the plasma flows caused by the resultant of the forces $\mathbf{f}^{(1)}$ and $\mathbf{f}_\perp^{(H)}$ would result in a plasma sheet inclined to the $y = 0$ plane by the angle Ψ, which is determined by the parameter χ_z and lies between 0° to 45°. Actually, this angle decreases with time and varies in space. Nevertheless, a change in the direction of the plasma flows in the early stage of the process would affect the spatial structure of the sheet that has already formed by that time.

Note that the Hall current exists until the plasma ions acquire a velocity close to the electron velocity in the (x, y) plane. Obviously, the greater the mass of an ion, the slower the process of ion acceleration. Since the Hall currents decay, the forces $\mathbf{f}_\perp^{(H)}$ should decrease with time and, accordingly, the shifts of the edges of the plasma sheet from the midplane $y = 0$ should also decrease. Hence, the greater the mass of a plasma ion, the slower should be a decrease in the sheet tilt relative to the $y = 0$ plane, as is actually observed in the experiment (see Fig. 8).

All this indicates that the deformation of a sheet is due to the generation of Hall currents and that the reduction in the sheet deformation with time is largely caused by the decay of Hall currents due to the acceleration of the plasma ions. For the lightest of the working gases (helium), the electron and ion velocities are equalized and, accordingly, the Hall currents decay well before the beginning of the sheet formation. Note that, in plasmas of heavier gases, the Alfvén time is longer; therefore, the current sheet forms at a slower rate and, accordingly, the magnetic field also varies more slowly (see [2, 3, 33]). This circumstance can also contribute to a change in the dependence $\Delta y(t)$ with increasing ion mass (see Fig. 8).

Another factor that may be responsible for this effect is a change in the plasma density and electron temperature and the corresponding change in the values of τ_e and the Hall parameter χ_z. Note, it is the appearance of plasma density inhomogeneities comparable with the sensitivity limit of holographic interferometry that makes it possible to study the structure of plasma sheets in the early stage of their formation (at $t \approx 1.5$–2 μs); i.e., all the experimental data presented in this paper were obtained under conditions such that the parameter χ_z was certainly nonuniform. Since χ_z is spatially nonuniform, the relative contributions from the forces $\mathbf{f}^{(1)}$ and $\mathbf{f}_\perp^{(H)}$ may be different in different regions of the sheet (e.g., in the central region and at the edge). This may lead to the experimentally observed curvature of the sheet in the early stage of its formation (see Figs. 2–4), when the sheet region located near the X line, where the plasma density is high enough, is almost parallel to the x axis, whereas the sheet edges are deflected from this axis by rather large angles.

That the shift of the side edges of a plasma sheet in the y direction decreases with time may also be attributed to the fact that the magnetic configuration varies during the formation of a current sheet. As a rule, the magnetic structure of current sheets in the quasi-steady stage of their evolution contains a singular X line (see [33]). However, the separatrix planes, which intersect at the X line, make rather small angles with the midplane of the sheet ($y = 0$) (Fig. 11), in contrast to the angles $\pi/4$ in initial magnetic field (1) (Figs. 10a, 10b). This is because the tangential component of the magnetic field, B_x, increases substantially, whereas the component B_y, which is normal to the sheet, decreases as compared to that in initial field (1). Thus, we have $B_x \approx 2.5$–3 kG near the sheet surface (i.e., $B_x/B_x^0 \approx 8$–10), whereas

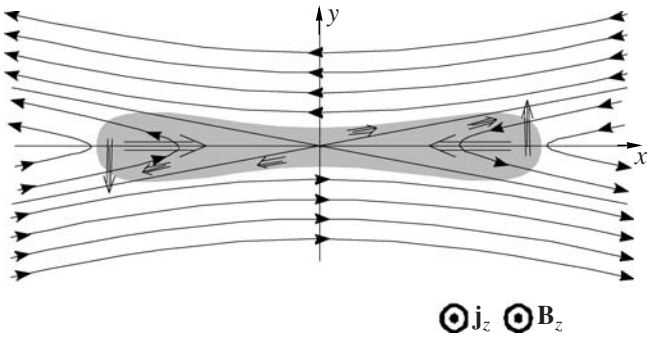

Fig. 11. Structure of the magnetic field $\mathbf{B}_\perp$ in the quasi-steady stage of the sheet evolution; the Hall currents; and the forces $\mathbf{f}_\perp^{(H)}$, arising due to the interaction of the Hall currents with the longitudinal magnetic field $\mathbf{B}_Z$. The current sheet is shown by shades of gray, the lines of the transverse magnetic field are shown by light solid lines, the Hall currents are shown by double arrows, and the forces $\mathbf{f}_\perp^{(H)}$ within the current sheet are shown by solid arrows.

$B_y/B_y^0 \approx 0.3$. It follows from expression (3) that the forces $\mathbf{f}^{(1)}$, which act in the (x, y) plane and arise due to the interaction of the main (longitudinal) current $\mathbf{j}_z$ with the transverse magnetic field $\mathbf{B}_\perp$, should be directed perpendicular to the magnetic field $\mathbf{B}_\perp$. If conditions for the excitation of the Hall currents $\mathbf{j}^{(H)}$ are satisfied, these currents must be parallel but oppositely directed to the forces $\mathbf{f}^{(1)}$ (see Eq. (7a)). The interaction of the Hall currents $\mathbf{j}^{(H)}$ with the longitudinal magnetic field $\mathbf{B}_z$ gives rise to the forces $\mathbf{f}_\perp^{(H)}$, which are antiparallel to the magnetic field $\mathbf{B}_\perp$ (when $\mathbf{j}_z$ and $\mathbf{B}_z$ have the same directions) (see expression (9a) and Fig. 11) or coparallel to this field (when $\mathbf{j}_z$ and $\mathbf{B}_z$ are directed oppositely).

We emphasize that the current density $\mathbf{j}_z$ in the formed sheet is concentrated in a relatively thin region of size $2\delta y \approx 1$–2 cm. According to Eqs. (7), it is in this region that the Hall currents directed predominantly along the x axis can be excited (see Fig. 11). In this stage, the plasma sheet can deform due to the interaction of the Hall currents with the longitudinal magnetic field $\mathbf{B}_z$, as was previously shown in our works [4, 10].

Thus, the main results obtained in studying the structure of current sheets formed in 3D magnetic field with an X line (1) can be satisfactorily explained by taking into consideration the Hall currents generated in the plasma. It should be noted that it is the longitudinal field $\mathbf{B}_z$ (in which plasma sheets become tilted and asymmetric) that allows one to reveal the Hall currents when studying the plasma structure by holographic interferometry.

4. CONCLUSIONS

The structure of plasma sheets formed in 3D magnetic configurations with a singular X line in the presence of a longitudinal component $\mathbf{B}_z$ directed along the X line has been studied experimentally.

It is found that the shape of a plasma sheet depends substantially on the mass of a plasma ion. Sheets produced in He are plane and symmetric, whereas those formed in plasmas of heavy noble gases (Ar, Kr, and Xe) are tilted and asymmetric. Characteristically, the tilt and asymmetry become more pronounced as the mass of a plasma ion increases.

It is shown that plasma sheets produced in plasmas of both light and heavy gases in the absence of a longitudinal magnetic field ($\mathbf{B}_z = 0$), i.e., in 2D magnetic configurations, are not tilted. The tilt increases with increasing absolute value of $\mathbf{B}_z$ and changes its sign when the direction of $\mathbf{B}_z$ is reversed. The tilt and asymmetry are mainly observed at the side edges of the sheets in the early stage of the sheet formation and then decrease with time.

The experimental data convincingly demonstrate that these effects are a manifestation of the two-fluid properties of the plasma containing heavy ions. The proposed qualitative model of plasma dynamics with allowance for the Hall effect explains most of the experimentally observed effects. In this model, the tilt and asymmetry of plasma sheets are attributed to additional forces associated with the interaction of the longitudinal magnetic field $\mathbf{B}_z$ with the Hall currents excited in a plane perpendicular to the X line.

The experimental results obtained in this study and their interpretation allow us to conclude that Hall currents contribute substantially to the plasma dynamics and the structure of current sheets formed in magnetic configurations with a singular X line. It is worth noting that, the excitation of Hall currents has been observed in a number of experiments that were carried out at different plasma densities, different configurations and strengths of the magnetic field, and different geometries and dimensions of the device (see, e.g., [17] and the references therein). Furthermore, space experiments performed with a series of *Cluster* satellites directly indicate the excitation of Hall currents in the Earth's magnetosphere [42]. Numerical simulations with allowance for Hall currents yield more realistic velocities of magnetic reconnection in current sheets [24].

In the present study, experimental data on the dynamics and structure of plasma sheets formed in 3D magnetic configurations with an X line were obtained by processing holographic interferograms. Hence, the method of holographic interferometry proves to be very efficient in such studies. An important advantage of this method is that it allows one to observe the 2D structure of plasma sheets and their evolution in time and space. However, holographic interferometry does not give direct information on the Hall currents and can confirm

their existence only indirectly by observing how the structure of a plasma sheet varies in the presence of a longitudinal magnetic field. Therefore, the results of recent direct measurements of Hall currents in magnetic configurations with an X line are of particular interest [43].

ACKNOWLEDGMENTS

This work was supported by the International Science and Technology Center (project no. 2098), the Russian Foundation for Basic Research (project no. 06-02-17011), and the RF Presidential Program for State Support of Leading Scientific Schools (project no. NSh-5382.2006.2).

REFERENCES

1. S. I. Syrovatskii, Ann. Rev. Astron. Astrophys. **19**, 163 (1981).
2. A. G. Frank, S. Yu. Bogdanov, V. S. Markov, et al., Phys. Plasmas **12**, 052 316 (2005).
3. S. Yu. Bogdanov, G. V. Dreĭden, V. S. Markov, et al., Fiz. Plazmy **32**, 1121 (2006) [Plasma Phys. Rep. **32**, 1034 (2006)].
4. A. G. Frank, S. Yu. Bogdanov, G. V. Dreiden, et al., in *Proceedings of the 30th EPS Conference on Controlled Fusion and Plasma Physics, St-Petersburg, 2003,* ECA **27A**, P-1.35 (2003).
5. A. G. Frank, S. Yu. Bogdanov, S. G. Bugrov, et al., Bull. Am. Phys. Soc. **49** (8), 29 (2004).
6. G. V. Dreiden, N. P. Kyrie, V. S. Markov, et al., Fiz. Plazmy **3**, 45 (1977) [Sov. J. Plasma Phys. **3**, 26 (1977)].
7. S. Yu. Bogdanov, G. V. Dreiden, A. G. Frank, et al., Physica Scr. **30**, 282 (1984).
8. S. Yu. Bogdanov, G. V. Dreiden, N. P. Kyrie, et al., Fiz. Plazmy **18**, 1269 (1992) [Sov. J. Plasma Phys. **18**, 654 (1992)].
9. S. Yu. Bogdanov, V. S. Markov, A. G. Frank, et al., Fiz. Plazmy **28**, 594 (2002) [Plasma Phys. Rep. **28**, 594 (2002)].
10. A. G. Frank, S. Yu. Bogdanov, G. V. Dreiden, et al., Phys. Lett. A **348**, 318 (2006).
11. G. Ostrovskaya, A. Frank, S. Bogdanov, et. al., in *Proceedings of the International Conference "Holography 2005," Varna, 2005*, Proc. SPIE **6252**, 625 228 (2006).
12. A. G. Frank, S. Yu. Bogdanov, S. G. Bugrov, et al., in *Proceedings of the 13th International Conferernce on Plasma Physics, Kiev, 2006*, Paper A008o.
13. R. L. Stenzel and W. Gekelman, J. Geophys. Res. **86**, 649 (1981).
14. Y. Yagi and N. Kawashima, Jpn. J. Appl. Phys. **24**, L259 (1985).
15. C. D. Cothram, M. Landerman, and M. R. Brown, Geophys. Rev. Lett. **32**, L03 105 (2005).
16. Y. Ren, M. Yamada, S. Gerhardt, et al., Phys. Rev. Lett. **95**, 055 003 (2005).
17. M. Yamada, Y. Ren, H. Ji, et al., Phys. Plasmas **13**, 052 119 (2006).
18. V. M. Vasyliunas, Rev. Geophys. Space Phys. **13**, 303 (1975).
19. B. U. O. Sonnerup, in *Solar System Plasma Physics*, Ed. by L. T. Lanzerotti, C. F. Kannel, and E. N. Parker (North-Holland, Amsterdam, 1979), p. 46.
20. T. Terasawa, Geophys. Rev. Lett. **10**, 475 (1983).
21. J. F. Drake and G. R. Burkhart, Geophys. Rev. Lett. **19**, 1077 (1992).
22. D. Biscamp, E. Schwarz, and J. F. Drake, Phys. Rev. Lett. **75**, 3850 (1995).
23. S. V. Bulanov, G. I. Dudnikova, V. P. Zhukov, et al., Tr. Inst. Obshch. Fiz., Ross. Akad. Nauk **51**, 101 (1996).
24. J. Birn, J. F. Drake, M. A. Shay, et al., J. Geophys. Res. **106**, 3715 (2001).
25. P. L. Pritchett and F. V. Coronity, J. Geophys. Res. **109**, A01 220 (2004).
26. P. Ricci, J. U. Brackbill, W. Daughton, and G. Lapenta, Phys. Plasmas **11**, 4102 (2004).
27. S. Yu. Bogdanov, N. P. Kyrie, V. S. Markov, and A. G. Frank, Pis'ma Zh. Éksp. Teor. Fiz. **71**, 72 (2000) [JETP Lett. **71**, 53 (2000)].
28. A. G. Frank and S. Yu. Bogdanov, Earth Planets Space **53**, 531 (2001).
29. A. G. Frank, Plasma Phys. Controlled Fusion **41** (Suppl. 3A), A687 (1999).
30. S. I. Syrovatskii, Zh. Éksp. Teor. Fiz. **50**, 1133 (1966) [Sov. Phys. JETP **23**, 754 (1966)].
31. S. I. Syrovatskii, Astron. Zh. **43**, 340 (1966) [Sov. Astron. J. **10**, 270 (1966)].
32. S. I. Syrovatskii, A. G. Frank, and A. Z. Khodzhaev, Pis'ma Zh. Éksp. Teor. Fiz. **15**, 138 (1972) [JETP Lett. **15**, 94 (1972)].
33. S. Yu. Bogdanov, S. G. Bugrov, V. P. Gritsyna, et al., Fiz. Plazmy **33**, 483 (2007) [Plasma Phys. Rep. **33**, 435 (2007)].
34. A. G. Frank, Tr. Fiz. Inst. im. P. N. Lebedeva, Ross. Akad. Nauk **74**, 108 (1974).
35. D. A. Frank-Kamenetskii, *Course of Plasma Physics* (Atomizdat, Moscow, 1968) [in Russian].
36. B. B. Kadomtsev, *Collective Phenomena in Plasma* (Nauka, Moscow, 1976) [in Russian].
37. A. S. Kingsep, K. V. Chukbar, and V. V. Yan'kov, in *Reviews of Plasma Physics*, Ed. by B. B. Kadomtsev (Énergoatomizdat, Moscow, 1987; Consultants Bureau, New York, 1990), Vol. 16.
38. D. Biscamp, *Magnetic Reconnection in Plasmas* (Cambridge Univ. Press, Cambridge, 2000).
39. A. S. Kingsep, *Introduction to Nonlinear Plasma Physics* (MZ-PRESS, Moscow, 2004) [in Russian].
40. E. R. Priest and T. Forbes *Magnetic Reconnection: MHD Theory and Applications* (Cambridge Univ. Press, Cambridge, 2000; Fizmatlit, Moscow, 2005).
41. A. I. Morozov, *Introduction to Plasmodynamics* (Fizmatlit, Moscow, 2006) [in Russian].
42. F. S. Mozer, S. D. Bale, and T. D. Phan, Phys. Rev. Lett. **89**, 015 002 (2002).
43. A. G. Frank, S. G. Bugrov, and V. S. Markov, in *Proceedings of the XXVIII International Conference on Phenomena in Ionized Gases, Prague, 2007*, p. 362.

Translated by N.F. Larionova